

# LiSb<sub>3</sub>O<sub>8</sub>: the first tetra rutile structure†

M. Elmina Lopes,<sup>a</sup> Caroline A. Kirk,<sup>a</sup> Susan M. Blake,<sup>b</sup> James Marr<sup>b</sup> and Anthony R. West<sup>a</sup>

<sup>a</sup> University of Sheffield, Department of Engineering Materials, Mappin Street, Sheffield, UK S1 3JD.  
E-mail: a.r.west@sheffield.ac.uk

<sup>b</sup> University of Aberdeen, Department of Chemistry, Meston Walk, Aberdeen, UK AB24 3UE

Received (in Cambridge, UK) 21st July 2000, Accepted 1st September 2000

First published as an Advance Article on the web

The new phase, LiSb<sub>3</sub>O<sub>8</sub>, synthesised by solid state reaction at 900 °C, has an ordered rutile structure with 1:3 cation order and monoclinic symmetry:  $a = 10.2578(9)$ ,  $b = 4.7063(3)$ ,  $c = 5.6017(5)$  Å,  $\beta = 96.467(7)^\circ$ , space group  $P2_1/a$ .

The rutile structure is found in a variety of oxides (e.g. TiO<sub>2</sub>, SnO<sub>2</sub>) and halides (e.g. MgF<sub>2</sub>). More complex, ordered rutile structures with 1:1 cation order occur in dirutiles (e.g. CoReO<sub>4</sub>), although with different cation arrangements, and with 1:2 order in trirutiles (e.g. ZnSb<sub>2</sub>O<sub>6</sub>).<sup>1</sup> We present here, the first example of 1:3 cation order in the new phase LiSb<sub>3</sub>O<sub>8</sub>, the structure of which can therefore be described as a tetra rutile.

LiSb<sub>3</sub>O<sub>8</sub> is a thermodynamically stable phase, synthesised by solid state reaction of Li<sub>2</sub>CO<sub>3</sub> and Sb<sub>2</sub>O<sub>3</sub> powder mixtures in Pt foil boats in air, initially at 700 °C for 2 h to expel CO<sub>2</sub> and finally at 900 °C for 2–3 days, with intermittent regrinding. The powder X-ray diffraction (XRD) pattern (Stoe Stadi diffractometer, Cu-Kα<sub>1</sub> radiation) was indexed by trial-and-error, using the TREOR program in the Stoe software package, on a monoclinic unit cell,  $a = 10.2578(9)$ ,  $b = 4.7063(3)$ ,  $c = 5.6017(5)$  Å,  $\beta = 96.467(7)^\circ$ . The first 20 indexed lines are given in Table 1. A search through both the International Centre for Diffraction Data file and the Inorganic Crystal Structure Database did not reveal any similar powder pattern or unit cell and therefore, LiSb<sub>3</sub>O<sub>8</sub> probably had a previously unreported structure type.

The structure was determined *ab initio* using the EXPO software package. First, the Sb positions were located by direct methods. Refinement of the partial structure (Sb only) was then carried out using the program GSAS followed by difference Fourier analysis to locate the oxygen atoms. At this stage, a drawing of the crystal structure was made which showed the existence of octahedral sites for Sb within an oxygen array that approximated to hexagonal close packed. Additional octahedrally coordinated sites, which corresponded to positions with some residual electron density in a difference map, were located and assigned to Li. The structure converged fully upon Rietveld refinement of the XRD data with the final coordinates given in Table 2. The refinement was entirely satisfactory apart from the  $U_{iso}$  value for Li, which refined to a slightly negative value and was therefore fixed at 0.025 in the final stages of refinement. This could indicate difficulties in the refinement of the light atom Li in the presence of Sb or a small amount of cross-substitution ( $\leq 1\%$ ) between Li and Sb sites so as to increase the effective electron concentration on the Li sites. Neutron diffraction studies are planned to resolve this question.

Bond lengths and a selection of bond angles are given in Table 3 (ESI†); projections of the structure are given in Fig. 1 and a profile fit is shown in Fig. 2 (ESI†). The structure has a rutile-like subcell, with a supercell caused by 1:3 ordering of Li:Sb on octahedral sites in the columns of edge-sharing octahedra parallel to  $c$  in the rutile subcell;  $V_{supercell} = 4V_{subcell}$ ;  $Z = 2$ ;  $a_{supercell}/[102]_{subcell}$ ;  $c_{supercell}/[10\bar{1}]_{subcell}$ .  $ac$  Projections of the subcell and supercell are shown in Fig. 1(a) as dotted and continuous lines, respectively. The columns of edge-sharing octahedra run vertically in the plane in Fig. 1(a) and therefore, run obliquely through the supercell. These columns are seen edge-on in Fig. 1(b), as a  $[10\bar{1}]$  projection of the

† Electronic supplementary information (ESI) available: Fig. 2: experimental, calculated and difference XRD profiles. Table 3: bond lengths and selected bond angles for LiSb<sub>3</sub>O<sub>8</sub>. Table 4: oxygen–oxygen distances in LiSb<sub>3</sub>O<sub>8</sub>. See <http://www.rsc.org/suppdata/cc/b0/b005915n/>

**Table 1** Indexed X-ray powder diffraction data for LiSb<sub>3</sub>O<sub>8</sub>

$2\theta_{obs}/^\circ$	$h$	$k$	$l$	$2\theta_{calc}/^\circ$	$\Delta(2\theta)$	$d_{obs}/\text{Å}$	$d_{calc}/\text{Å}$	$I_{obs}$	$I_{calc}$
15.892	0	0	1	15.910	−0.018	5.5722	5.5660	13	12
17.370	2	0	0	17.387	−0.017	5.1012	5.0963	15	14
20.759	1	1	0	20.772	−0.013	4.2754	4.2728	18	18
22.256	−2	0	1	22.267	−0.011	3.9911	3.9892	13	11
24.743	0	1	1	24.754	−0.011	3.5954	3.5938	4	1
24.941	2	0	1	24.963	−0.022	3.5672	3.5641	8	7
25.644	−1	1	1	25.657	−0.012	3.4710	3.4693	12	11
26.867	1	1	1	26.877	−0.010	3.3157	3.3145	100	100
29.320	−2	1	1	29.326	−0.006	3.0436	3.0431	2	<1
31.454	2	1	1	31.461	−0.007	2.8419	2.8413	2	<1
32.133	0	0	2	32.137	−0.004	2.7833	2.7830	4	3
32.473	3	1	0	32.476	−0.004	2.7550	2.7547	7	7
34.956	−2	0	2	34.922	0.034	2.5647	2.5672	50	17
	−3	1	1	34.971	−0.015		2.5637		35
35.186	4	0	0	35.192	−0.006	2.5485	2.5481	20	17
37.091	−4	0	1	37.082	0.009	2.4219	2.4225	2	1
37.698	−1	1	2	37.702	−0.004	2.3843	2.3840	9	6
	3	1	1	37.705	−0.007		2.3839		3
38.213	0	2	0	38.216	−0.003	2.3533	2.3531	9	9
38.521	2	0	2	38.534	−0.013	2.3352	2.3344	9	9
39.289	1	2	0	39.262	0.027	2.2913	2.2928	2	<1
39.422	1	1	2	39.434	−0.013	2.2839	2.2832	2	1

**Table 2** Atomic positions and isotropic thermal parameters for  $\text{LiSb}_3\text{O}_8$ 

Atom	Site	<i>x</i>	<i>y</i>	<i>z</i>	Site occupancy	$U_{\text{iso}}$
Sb(1)	4e	0.25108(7)	−0.47980(2)	0.2375(1)	1	1.33(2)
Sb(2)	2b	0.5	0	0.5	1	1.34(3)
O(1)	4e	0.3266(7)	−0.774(2)	0.477(2)	1	1.6(2)
O(2)	4e	0.4210(7)	−0.291(2)	0.276(2)	1	0.8(2)
O(3)	4e	0.8264(7)	0.192(2)	−0.013(2)	1	1.0(2)
O(4)	4e	0.5799(7)	0.174(1)	0.230(2)	1	1.3(2)
Li	2a	0	0	0	1	0.025 <sup>a</sup>

<sup>a</sup> Not refined; default value used.  $\chi^2 = 3.168$ ,  $R_{\text{wp}} = 10.05\%$ ,  $R_{\text{p}} = 7.76\%$ .

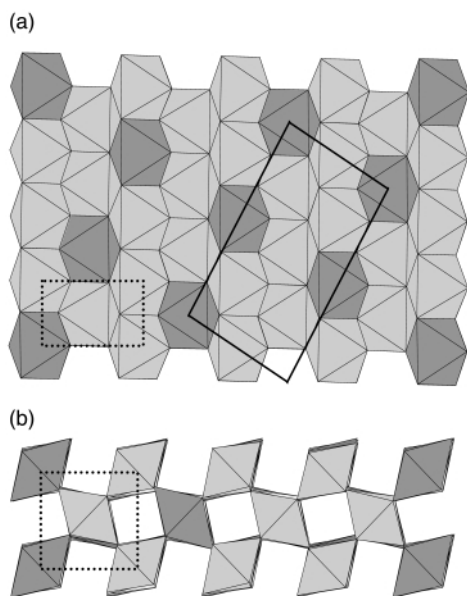


**Fig. 1** Projections of the  $\text{LiSb}_3\text{O}_8$  structure. Dark octahedra:  $\text{LiO}_6$ ; light octahedra:  $\text{SbO}_6$ . (a) Projection in the *ac* plane showing subcell (dotted) and supercell (continuous); (b) projection down  $[10\bar{1}]$  showing columns of edge-sharing octahedra with corrugated *tp* oxide layers running horizontally and vertically.

supercell. As with rutile, edge-sharing of octahedra leads to structural distortion associated with cation repulsion effects and this reduces the O–Sb–O and O–Li–O angles facing the shared edges to *ca.* 80° (Table 3). Li–O and Sb–O distances are in the ranges 1.99–2.11 and 1.95–2.10 Å, respectively, giving very similar sized  $\text{LiO}_6$  and  $\text{SbO}_6$  octahedra.

The structure may be described in two rather different ways: either as filling of half the octahedral sites in a distorted hexagonal close packed (*hcp*) oxide array; or, as filling of all the (undistorted) octahedral sites in a tetragonal packed (*tp*) array.<sup>2,3</sup> The latter viewpoint is a more accurate description; although the structure does not possess fourfold symmetry (unlike the parent rutile structure), the corrugated *tp* layers are seen running horizontally and vertically in Fig. 1(b), together with the diamond-shaped (in projection) columns of edge-sharing octahedra and the square-shaped columns containing empty distorted tetrahedral and distorted octahedral interstitial sites. The *tp* nature of the oxide ion array is further demonstrated by consideration of the oxygen–oxygen closest distances. In *hcp*, 12 equidistant oxygens are expected; in *tp*, ideally there are 11 equidistant oxygens, plus 2 somewhat

further away. The distribution of distances in  $\text{LiSb}_3\text{O}_8$  clearly falls into the second category (Table 4, ESI†): for the four crystallographically distinct oxygens, there are 11 O–O distances in the range 2.60–3.13 Å and 2 O–O distances at 3.34–3.49 Å; the next shortest O–O distances are at 3.92 Å.

Antimonates are often isostructural with compositionally similar niobates and tantalates. The rutile-related structure of  $\text{LiSb}_3\text{O}_8$  is, however, distinct from that of both  $\text{LiNb}_3\text{O}_8$  and  $\text{LiTa}_3\text{O}_8$ .  $\text{LiNb}_3\text{O}_8$  has a cation-ordered  $\alpha$ - $\text{PbO}_2$  structure in which cations occupy half the octahedral sites in an *hcp* oxide array.<sup>4,5</sup> The distribution of occupied octahedral sites gives rise to zigzag chains of edge-sharing octahedra, rather than the linear chains in  $\text{LiSb}_3\text{O}_8$  and other rutile derivatives; also the oxide array is *hcp* instead of *tp*.  $\text{LiTa}_3\text{O}_8$  exists in three polymorphic forms. The L polymorph is isostructural with  $\text{LiNb}_3\text{O}_8$ .<sup>5</sup> The M polymorph also has an  $\alpha$ - $\text{PbO}_2$  superstructure but with a different cation arrangement to that of the L polymorph<sup>6,7</sup> and is isostructural with the mineral wadginite. The structure of the H polymorph is quite different and contains a mixture of  $\text{TaO}_7$  pentagonal bipyramids and  $\text{TaO}_6$  octahedra.<sup>8–12</sup>

$\text{LiSb}_3\text{O}_8$  is the first rutile derivative structure with 1:3 cation order and may therefore be described as a tetrarutile. It is possible that other  $\text{M}(\text{i})\text{M}(\text{v})_3\text{O}_8$  phases may have the same structure (although not with  $\text{LiNb}_3\text{O}_8$  and  $\text{LiTa}_3\text{O}_8$ , apparently). It is also possible that other tetrarutile structures may form with different cation arrangements, in the same way that different dirutile cation arrangements exist.<sup>1</sup>

## Notes and references

- W. H. Baur, *Z. Kristallogr.*, 1994, **209**, 143.
- W. H. Baur, *Mater. Res. Bull.*, 1981, **16**, 339.
- A. R. West and P. G. Bruce, *Acta Crystallogr., Sect. B*, 1982, **38**, 1891.
- M. Lundberg, *Acta Chem. Scand.*, 1971, **25**, 3337.
- B. M. Gatehouse and P. Leverett, *Cryst. Struct. Commun.*, 1972, **1**, 83.
- B. M. Gatehouse, T. Negas and A. S. Roth, *J. Solid State Chem.*, 1976, **18**, 1.
- A. Santoro, A. S. Roth and D. Minor, *Acta Crystallogr., Sect. B*, 1977, **33**, 3945.
- A. G. Nord and J. O. Thomas, *Acta Chem. Scand. Ser. A*, 1978, **32**, 539.
- P. E. Werner, B. O. Marinder and A. Magneli, *Mater. Res. Bull.*, 1978, **13**, 1371.
- G. D. Fallon, B. M. Gatehouse, R. S. Roth and A. S. Roth, *J. Solid State Chem.*, 1979, **27**, 255.
- M. Pouchard and J. P. Chaminade, *Compt. Rend. Acad. Seances – Ser. C*, 1972, **274**, 1739.
- J. L. Houdeau, M. Marezio, A. Santoro and A. S. Roth, *J. Solid State Chem.*, 1984, **51**, 275.